Gutiérrez-Tarriño, S.; Rojas-Buzo, S.; Lopes, CW.; Agostini, G.; Calvino, JJ.; Corma Canós, A.; Oña-Burgos, P. (2021). Cobalt nanoclusters coated with N-doped carbon for chemoselective nitroarene hydrogenation and tandem reactions in water. Green Chemistry. 23(12):4490-4501. https://doi.org/10.1039/d1gc00706h

Cobalt Nanoclusters Coated by N-Doped Carbon for Chemoselective Nitroarene Hydrogenation and Tandem Reactions in Water

Silvia Gutiérrez-Tarriño,[a] Sergio Rojas-Buzo,[a] Christian W. Lopes,[b] Giovanni Agostini,[c] Jose. J. Calvino,[d,e] Avelino Corma[a] and Pascual Oña-Burgos[a,f*]

[a]*Instituto de Tecnología Química, Universitat Politècnica de València-Consejo Superior de Investigaciones Científicas (UPV-CSIC), Avda. de los Naranjos s/n, 46022 Valencia, Spain.*

[b]*Institute of Chemistry, Universidade Federal do Rio Grande do Sul – UFRGS, Av. Bento Gonçalves, 9500, 91501-970 Porto Alegre, RS, Brazil.*

[c]*CELLS-ALBA Synchrotron Radiation Facility, 08290 Cerdanyola del Valles, Barcelona, Spain.*

[d]*Departamento de Ciencia de los Materiales e Ingeniería Metalúrgica y Química Inorgánica, Facultad de Ciencias, Universidad de Cádiz, Campus Río San Pedro S/N, Puerto Real 11510, Cádiz, Spain.*

[e]*Instituto Universitario de Investigación de Microscopía Electrónica y Materiales (IMEYMAT), Facultad de Ciencias, Universidad de Cádiz, Campus Río San Pedro S/N, Puerto Real 11510, Cádiz, Spain*

[f]*Department of Chemistry and Physics, Research Centre CIAIMBITAL, University of Almería, Ctra. Sacramento, s/n, 04120 Almería, Spain.*

ABSTRACT

The development of active and selective non-noble metal-based catalysts for the chemoselective reduction of nitrocompounds able to work in aquo media under mild conditions is an attractive research area. Herein, the synthesis of subnanometric and stable cobalt nanoclusters cover by N-doped carbon layers as core-shell (**Co@NC-800**) for the chemoselective reduction of nitroarenes is reported. The **Co@NC-800** catalyst was prepared by the pyrolysis of $Co(tpy)_2$ complex impregnated on vulcan carbon. In fact, the employment of a molecular complex based on six N-Co bounds drives the formation of a well-defined and distributed cobalt core-shell nanoclusters cover by N-doped carbon layers. In order to elucidate its nature this has been fully characterized by employing several advanced techniques. In addition, this as-prepared catalyst showed high activity, chemoselectivity and stability toward the reduction of nitrocompounds

with H_2 under mild reaction conditions and water as a green solvent, improving the previously results based on cobalt catalysts. Moreover, **Co@NC-800** catalyst is also active and selective for the one-pot synthesis of secondary aryl amines and isoindolinones through the reductive amination of nitroarenes. Finally, based on diffraction and spectroscopic studies, metallic cobalt nanoclusters with surface CoN_x patches have been proposed as the active phase in **Co@NC-800** material.

1. INTRODUCTION

The reduction of nitroarenes is an important process for the production of anilines and, in particular, their functionalized derivatives, which are key organic intermediates for manufacturing dyes, agrochemicals, pigments, pharmaceuticals and polymers.[1–3] In addition, they also represent essential building blocks for the preparation of novel highly valuable organic compounds as they can easily undergo further derivatization reactions.[4,5]

Owing to their immense utility, the development of novel catalysts for the synthesis of anilines remains an active research area. Among all known developed catalytic methods, direct reduction of nitroarenes catalyzed by noble metal catalysts, such as Au and Pt, with molecular hydrogen represents the most straightforward and atom-economy process.[6–12] However, considering the high price and limited availability of noble metals, it is interesting to develop non-noble metal catalysts for this reaction.

Among non-precious metals, nickel-based catalysts are the most used for the hydrogenation of several functional groups.[2,13,14] Nickel catalysts usually present several drawbacks, such as they are very sensitive, delicate to control, require very harsh reaction conditions, and end with low selectivity and recyclability.[2] However, in 2008, our group developed a TiO_2-supported Ni-based catalyst able to carry out this chemoselective hydrogenation with good activity under mild reaction conditions.[15] In the same way, iron catalysts also have these similar drawbacks.[16] On the other hand, although it has been demonstrated that cobalt catalysts are active for this reaction, their synthesis and utility are challenging and require severe reduction conditions to obtain metal nanoparticles. For this reason, many efforts have been made to improve the synthetic procedure.[2] In fact, it is known that the activity of a cobalt catalyst depends on the particle size and the nature of the support.[17] Moreover, it was reported that larger particles with a size of >10nm are the most active since smaller particles can be easily oxidized in the presence of air.[17] To avoid oxidation of the Co nanoparticles, our group has employed a straightforward methodology to cover medium-size cobalt nanoparticles (NPs) with carbon by thermal decomposition of Co-EDTA complex or by a simple carbon coating process based on hydrothermal treatment with glucose.[18,19] The nature and surface of the support also play an important role in the metal dispersion and final particle size.[17,20] In this sense, nitrogen-doped

heterogeneous supports were extensively used to stabilize the metal particles and obtain a better metal distribution.[20–25] In addition, nitrogen-rich supports also promote heterolytic hydrogen cleavage under milder conditions.[20] In this context, several independent research groups such as Beller,[26–28] Kempe,[29] Gascon,[30] and Yang[31] have developed numerous N-doped carbon modified cobalt-based catalysts for selective hydrogenation of functionalized nitroarenes (Scheme 1).

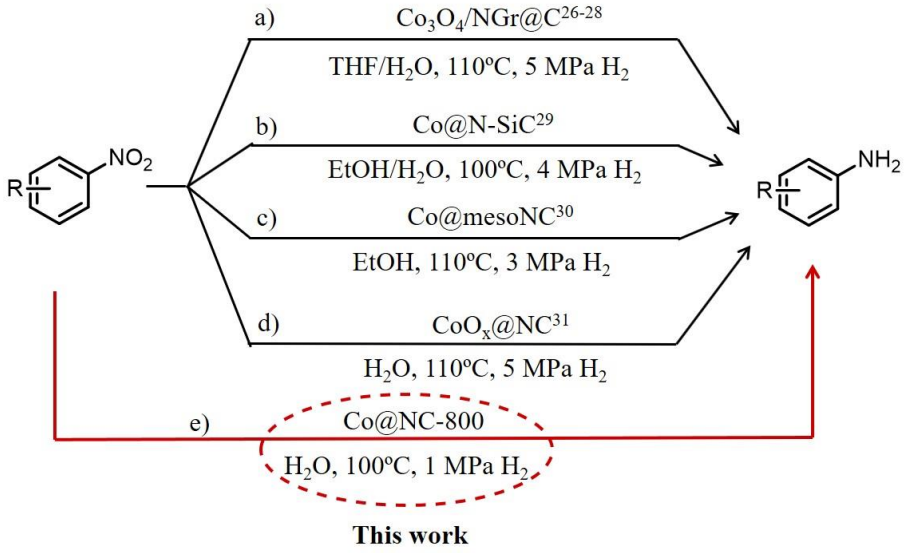

Scheme 1. Hydrogenation of nitroarenes over cobalt-based heterogeneous catalysts.

Despite the great achievements, non-green solvents or severe reaction conditions are necessary to achieve high conversions and selectivities (Scheme 1a-d). Therefore, there is still a great need to develop highly efficient and environmentally friendly methods to convert nitro compounds into amines selectively.

On the other hand, our group has promoted a selective and active catalytic system for the one-pot cascade type reactions, which avoids the isolation and purification of intermediates.[32] For instance, the reductive amination of carbonyl groups with a primary amine using Pd/C[33–36] offers a direct and selective way to secondary amines. Thus, recently, the development of efficient and selective methods through transition metal-catalyzed reductive amination has been actively explored.[28,29,37–40] Especially, much interest has been focused on finding an effective catalyst that can catalyze both the hydrogenation of nitro compounds and the reductive amination of the resulting amines in the presence of an aldehyde without being accompanied by unwanted side products.[41–48] Some of the challenges for this process are obtaining the amine product selectively instead of the imine, carry out the reaction under mild conditions and using green solvents, such as water, as the reaction media.

In this work, the utilization of terpyridine (tpy) as a ligand for $[Co(tpy)_2](NO_3)_2$ synthesis is set out, which is going to be immobilized in a carbon matrix. The final 1:2 complex with tpy ligand is formed since cobalt atoms surrounded by six nitrogen atoms will be more stabilized in the

carbon matrix than those with four nitrogen atoms. For this aim, it is necessary to use $Co(NO_3)_2 \cdot 6H_2O$ to form the homoleptic complex exclusively.[49] Interestingly, the as-prepared pyrolyzed cobalt material has shown high activity and excellent selectivity to reduce a wide range of nitroarenes under mild reaction conditions and water as a green solvent. Moreover, the obtained cobalt catalyst has also demonstrated high activity in tandem reactions such as the synthesis of secondary amines through the reductive amination of different nitroarenes and benzaldehyde and in the tandem reaction between several nitroarenes and 2-carboxybenzaldehyde to produce the desired oxoindolines. Besides, FTIR experiments were carried out to demonstrate the chemoselectivity of this catalyst in the 3-nitrostyrene reduction. Finally, the synthesized catalyst was characterized by several physicochemical techniques that elucidated the role of nitrogen and the active species in **Co@NC-800** material.

2. RESULTS AND DISCUSSION

2.1. Synthesis of catalysts

To carry out the synthesis of the heterogeneous catalysts, the homoleptic complex $Co(tpy)_2(NO_3)_2$ with 2 equivalents of 2,2':6',2''-terpyridine (Co:terpyridine = 1:2 molar ratio) was used as the cobalt source. For this aim, cobalt(II) nitrate hexahydrate and terpyridine were dissolved in ethanol. This complex was supported in the carbon matrix (Vulcan XC72R) through a wetness impregnation. Finally, the obtained material was pyrolyzed in a tubular vertical oven at different temperatures (400, 500, 600, 700 y 800ºC) (Scheme 2). The as-synthesized obtained catalysts were denoted as **Co@NC-T**, where NC represents the N-doped carbon matrix and T the pyrolysis temperature (see more details in the SI). For comparative purposes, the catalyst was also prepared in the absence of tpy ligand (**Co-P_1@NC-800** and **Co-P_2@NC-800**) and using alternative nitrogenated ligands such as 1,10-phenanthroline (**Co-L_2@NC-800**) and ethylenediaminetetraacetic acid (**Co-L_3@NC-800**).

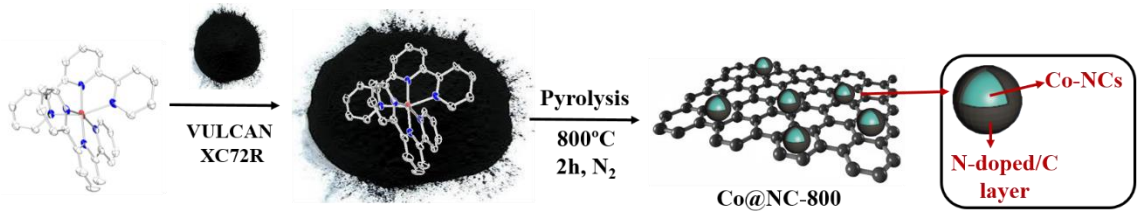

Scheme 2. Synthesis of catalysts **Co@NC-800** by pyrolysis of $[Co(tpy)_2](NO_3)_2$ complex on carbon.

2.2. Optimization of the reaction conditions

The as-prepared catalysts were tested for the catalytic hydrogenation of nitrobenzene as a benchmark reaction. The reaction was initially performed using standard conditions[26] based on Scheme 1 (110 ºC with 5.0MPa of H_2) with **Co@NC-800** as catalyst and different solvents to study the effect of the polarity of the reaction media on the catalytic activity (entries 1-4, Table 1). Interestingly, solvent effect has a strong influence on the reaction efficiency. Upon increasing the polarity of the reaction media, the conversion was enhanced, being water the solvent which showed the best catalytic performance with a complete conversion and high selectivity toward aniline.

In the second set of experiments, **Co@NC-T** catalysts obtained using different pyrolysis temperatures (400, 500, 600 and 700 ºC) were employed under the same reaction conditions (entries 5-8, Table 1). The catalyst that showed the best catalytic results was the one pyrolyzed at 800 ºC. So, the pyrolysis temperature for the resulting catalysts **Co@NC-T** has a considerable impact on the catalytic performance, which could be related to the nature of the metallic species promoted at each temperature. Moreover, different factors such as metal loading, solvent volume, H_2 pressure, and reaction temperature were considered in the hydrogenation of nitrobenzene when using **Co@NC-800** as catalyst (entries 9-18, Table 1). Fully conversion of nitrobenzene, with high selectivity to aniline, was observed even under mild reaction conditions. A decrease of H_2 pressure, maintaining the temperature and the metal loading (0.34 % w/w), led to a lower catalytic activity (entry 9). In the same way, the catalytic activity depends on the reaction temperature (entries 11-15, Table 1) with an increase of the efficiency with the temperature. However, complete conversion was obtained at 90 and 70 ºC, increasing the catalyst loading to 1.8% w/w (entries 12-13) after fourteen hours, being at 70 ºC (entry 13, Table 1) the softer conditions reported for this reaction with cobalt catalysts in aquo media to obtain these excellent values of activity and selectivity. Based on this optimization study together with a suitable ratio catalyst/feed, the catalytic conditions chosen for this reaction were 1MPa of H_2, 100 ºC and 1% mol of cobalt loading (30 mg of catalyst with 1% of metal loading). Interestingly, the kinetic profile of the reaction in Figure S1, indicates that nitrobenzene was converted smoothly into aniline and no intermediates were detected by gas chromatography during the entire reaction process.

Table 1. Optimization of reaction conditions[a]

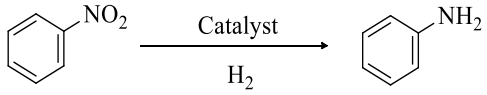

Entry	Catalyst	Solvent	P (MPa) H_2	T (ºC)	Co (%)[b]	Conversion(%)[c]	Selectivity (%)[c]
1	Co@NC-800	THF	5	110	0.34	15	>99
2	Co@NC-800	Toluene	5	110	0.34	25.8	>99
3	Co@NC-800	EtOH	5	110	0.34	97	>99
4	Co@NC-800	H_2O	5	110	0.34	>99	>99
5	Co@NC-400	H_2O	5	110	0.34	1.4	>99
6	Co@NC-500	H_2O	5	110	0.34	4.2	>99
7	Co@NC-600	H_2O	5	110	0.34	12.1	>99
8	Co@NC-700	H_2O	5	110	0.34	14	>99
9	Co@NC-800	H_2O	3	110	0.34	62.5	>99
10	Co@NC-800	H_2O	1	110	1	>99	>99
11	Co@NC-800	H_2O	1	90	1	76.5	>99
12	Co@NC-800	H_2O	1	90	1.8	>99	>99
13	Co@NC-800	H_2O	1	70	1.8	>99	>99
14	Co@NC-800	H_2O	1	50	1.8	34	>99
15	Co@NC-800	H_2O	1	Rt	1.8	12.5	>99
16	Co@NC-800[d]	H_2O	1	100	0.67	>99	>99
17	Co@NC-800[e][f]	H_2O	1	100	0.34	>99	>99
18	Co@NC-800	H_2O	1	100	1	>99	>99
19	Co-L_2@NC-800[g]	H_2O	1	100	1	65.4	>99
20	Co-L_3@NC-800[h]	H_2O	1	100	1	1.2	>99
21	Co-P_1@C-800[i]	H_2O	1	100	1	0	-
22	Co-P_2@C-800[j]	H_2O	1	100	1	0	-
23	Co_3O_4	H_2O	1	100	12.5	0	-
24	$Co(tpy)_2(NO_3)_2$	H_2O	1	100	10	0	-
25	C support[k]	H_2O	1	100	-	0	-
26	Blank	H_2O	1	100	-	0	-

[a]Reaction conditions: Nitrobenzene (0.5 mmol), solvent (3 mL), 14h. [b]Cobalt loading %w/w. [c]Determined by GC and GC-MS using hexadecane as an internal standard. [d]Solvent 2 mL, 20h of reaction time. [e]Solvent 1 mL, 20h of reaction time. [f]Nitrobenzene (1 mmol), solvent (20mL), 20h of reaction time. [g]L_2: 1,10-phenanthroline. [h]L_3: Ethylenediaminetetraacetic acid. [i]P_1: $Co(NO_3)_2 \cdot 6H_2O$. [j]P_2: $Co(acac)_2 \cdot H_2O$. [k]Pyrolyzed carbon.

For comparison, other cobalt complexes with nitrogenated ligands such as 1,10-phenanthroline (L_2) and ethylenediaminetetraacetic acid (L_3) were used as cobalt precursors (entries 19,20). Although **Co-L_2@NC-800** showed to be active in the nitrobenzene reduction, it is not as active

as **Co@NC-800** under optimized conditions. Moreover, the heterogeneous catalysts, **Co-P_1@C-800** and **Co-P_2@C-800** (without using any nitrogenated ligand, entries 21, 22), were also tested under optimized conditions. In both cases, aniline was not detected by GC chromatography during 14h, indicating that the N-dopant, which comes from the ligand, and the particle size, play an essential role in the final activity of the material and consequently in the activation of molecular hydrogen. To shed some light on the role of the nitrogen in the catalytic activity, the efficiency of **Co@NC-800**, **Co-L_2@NC-800** and **Co-P_1@C-800** in H/D exchange tests was compared. The isotopic exchange experiments showed that **Co@NC-800** dissociates H_2 faster than **Co-L_2@NC-800**, and that **CoP_1@C-800** does not dissociate H_2 in the same conditions. The ratio between mass signals HD/H_2 during the exchange experiments at reaction temperature (100 ºC) using **Co@NC-800** and **Co-L_2@NC-800** has a value of 0.09 and 0.062, respectively. The higher rate of **Co@NC-800** in the formation of HD is correlated with the higher heterolytic hydrogen cleavage, therefore, with a higher activity of the catalysts in hydrogenation reactions. Moreover, H_2 chemisorption studies over **Co@NC-800**, **Co-L_2@NC-800** and **Co-P_1@C-800** were also carried out to elucidate the number of active metal sites.[50] However, the H_2 chemisorption did not occur, which supports that this synthetic methodology promotes metal centers, which are not accessible once they are covered by N-doped carbon.

The presence of cobalt nanoclusters in the final catalyst is essential to carry out the reaction since no reactivity was observed in the absence of cobalt in the carbon support or in the presence of the cobalt complex $Co(tpy)_2(NO_3)_2$, or of pure nano Co_3O_4 as catalyst (entries 23-26, Table 1).

Finally, this reaction has been scaled up twenty times to 1 mmol of nitrobenzene (1.196 g) with an excellent result (> 99% of conversion and selectivity to aniline, entry 17f, Table 1).

2.3. Catalysts characterization.

All the catalysts synthesized in this study were characterized exhaustively by different techniques to better understanding the nature of cobalt species.

Considering that catalytic activity is correlated with pyrolysis temperature, the redox properties of **Co@NC-T** catalysts were studied by Temperature-Programmed Reduction (TPR). As shown in Figure S2, the H_2 consumption decreases as the pyrolysis temperature of the catalysts increases. Notably, the catalyst pyrolyzed at 800 ºC shows the lowest H_2 consumption among all the samples, suggesting a higher amount of reduced cobalt sites in this catalyst. This clearly supports our previous hypothesis that an increase in pyrolysis temperature drives the reduction of Co^{2+} species.

High-angle annular dark-field scanning transmission electron microscopy (HAADF-STEM) and energy-dispersive X-ray spectroscopy (EDX) investigations were conducted to understand in more detail the remarkable activity difference between **Co@NC-800** and the rest of the catalysts.

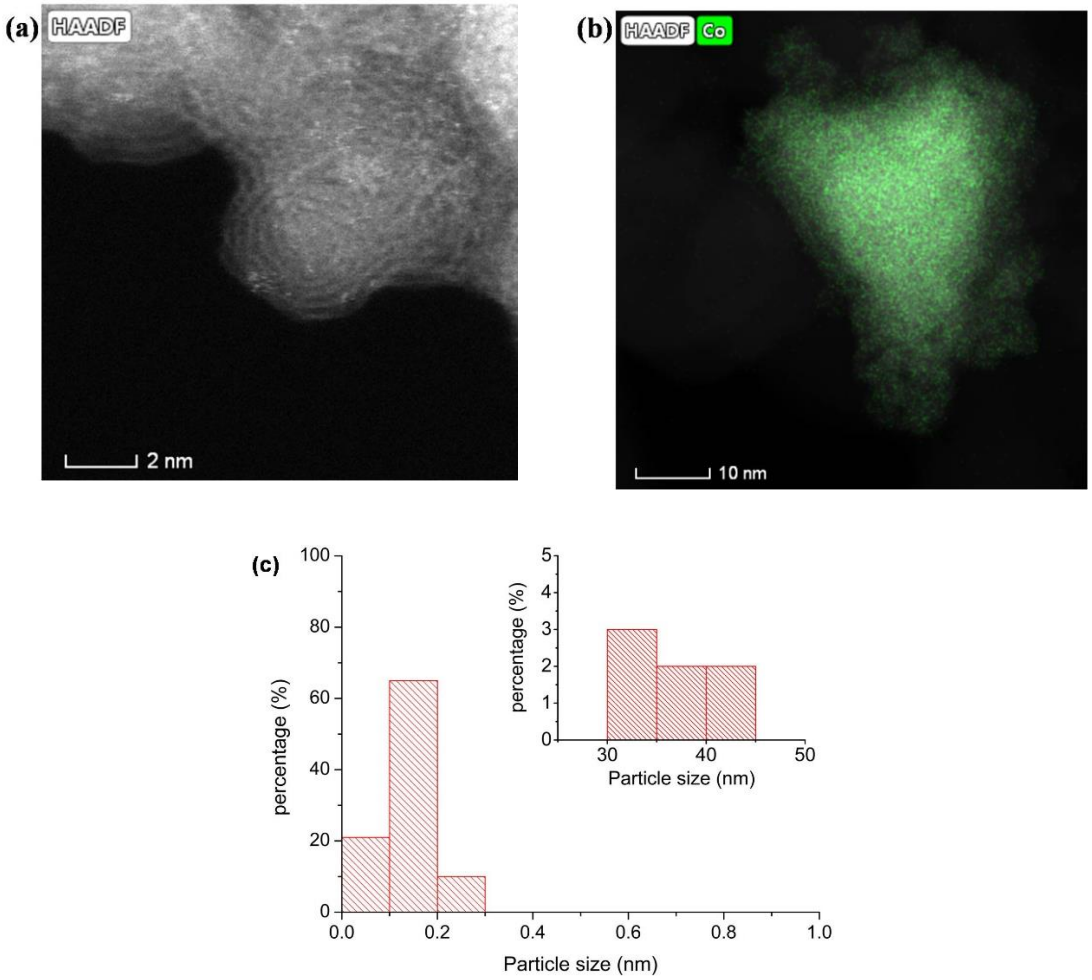

Figure 1. (a) HAADF-STEM image of **Co@NC-800.** The high-intensity bright spots correspond to Co atoms, (b) High-Resolution STEM-EDX map of **Co@NC-800.** The Co map has been overlayed on the STEM-HAADF image and (c) particle size distribution of **Co@NC-800** (200 particles counted). The inset shows the percentage of particles between 30 and 50 nm.

As shown in Figure S3, the particle size varies significantly with the pyrolysis temperature of the material. In the most active catalytic system, **Co@NC-800**, the particle size distribution is relatively wide (Figure 1c). This catalyst contains a large fraction of nanoclusters below 1 nm (Figure 1a) and a small contribution, around 7%, of aggregates in the range of 30-50 nm (Figure 1c, S3e). However, when the least active catalyst was analyzed, i.e. **Co@NC-400**, the size of the well-defined particles was larger than 200 nm (Figure S3). These results show that as the pyrolysis temperature increases, the amount of metal aggregates decreases so that

subnanometric nanoclusters are the main species after pyrolysis at 800ºC. Moreover, the particle size in the catalysts synthesized without using any nitrogenated ligands (**Co-P_1@C-800** and **Co-P_2@C-800)** was in the range of 10-20nm, also larger than in **Co@NC-800** (Figure S3f). These microscopy results fully support the initial catalytic test. Finally, the high dispersion and homogeneous distribution of Co in the carbon matrix of **Co@NC-800** was confirmed by high-resolution STEM-EDX analysis (Figure 1b). From these data, it could be concluded that the most active catalyst is the one depicting the highest metal dispersion (**Co@NC-800**) and more metallic character.

The XRD patterns shown in Figure S4a corresponding to the 7% of the Co aggregates of **Co@NC-800**, revealed that the main species present is metallic Co. Peaks at 44.0, 51.3 and 75.4 degrees, corresponding to (100), (200) and (220) crystal planes of structured metallic cubic cobalt[51] (JCPDS no. 15-0806), could be observed. It is worth noting that the peak at 2θ below 44º is characteristic of Co-N_x (JCPDS no. 41.0943).[52,53] In addition, the broad peak at around 25º is ascribed to the amorphous carbon-based support. These data are mainly used to compare the species present in the catalysts pyrolyzed at lower temperature with the ones present in **Co@NC-800**. In this sense, XRD patterns for **Co@NC-400** and **Co@NC-500** revealed that the main species present is CoO with broad peaks at 36.6 and 61.8 degrees, corresponding to (110) and (111) crystal planes of cubic CoO (JCPDS no. 001-1227).[54] For the other two materials, **Co@NC-600** and **Co@N-700**, a mixture of Co and CoO species is observed (Figure S4).

X-ray photoelectron spectroscopy (XPS) was employed to investigate the surface composition and the chemical state of the metal and the nitrogen in the **Co@NC-800** catalyst**.** Figure 2a proves that nitrogen is incorporated into the carbon matrix, indicating that the employed ligand participates in the generation of these materials.

Deconvolution of the N 1s spectrum (Figure 2a) gives rise to two peaks, this meaning that two types of N atoms are present. These correspond to N from NO_3^- (405.6 eV) and pyrrolic N or N coordinated to Co (Co-N_x centers) (399.8 eV).[56] Clearly, the peak assigned to pyrrolic or N coordinated to Co is the dominant one, serving as anchoring sites for Co atoms. Deconvolution revealed that around 74.9% of all nitrogen atoms are bound to the metal.[54]

Besides, the Co $2p_{3/2}$ XPS spectrum (Figure 2b) was fitted into three peaks at 778.7, 780.5 and 785.6 eV. The signal at 778.7 eV corresponds to metallic Co,[55] while the peak at 780.5 eV can be ascribed to Co-N_x species.[55–57] Finally, the signal at 785.6 matches the satellite peak of Co^{2+}.[55] This indicates that most of the Co atoms on the surface are present in the form of CoN_x.

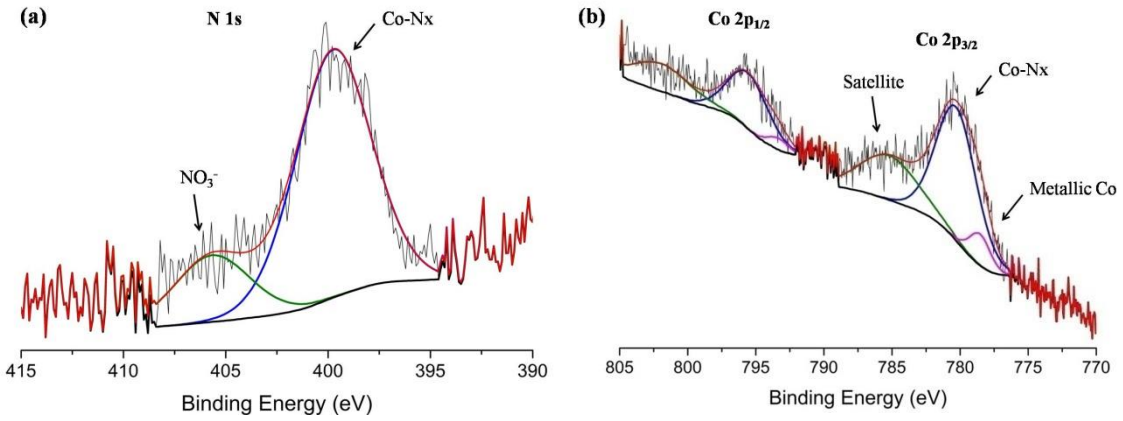

Figure 2. XPS Spectra of **Co@NC-800** (a) N 1s (b) Co 2p.

To confirm that bulk material structure matches with the surfaces analysis obtained by XPS, XAS study was also carried out. The normalized XANES spectra at Co K-edge of the cobalt precursor, $[Co(tpy)_2](NO_3)_2$, and **Co@NC-800** are shown in Figure 3. As expected, the cobalt precursor (Figure 3a) shows a similar edge position (~7720 eV) as for the $Co(OAc)_2$ standard, typical of Co^{2+}. Furthermore, non-centrosymmetric octahedral geometry for Co in the complex is inferred from the presence of a pre-edge peak at 7710 eV due to p-d hybridization of the Co atom orbitals with those of surrounding ligands.[58] The complex has different Co-N distances (Table S1), which reinforces its non-centrosymmetric character.

The XANES spectrum (Figure 3b) of **Co@NC-800** changes dramatically regarding the Co precursor. The edge position shifts to 7709 eV (similar to Co foil), demonstrating the reduction of Co^{2+} species to Co^0, which confirms the formation of Co nanoclusters. However, despite the similarity in edge position, the XANES features do not resemble those of metallic Co completely. Specifically, the higher intensity of the whiteline in **Co@NC-800** spectrum in comparison to the Co foil suggests some degree of Co oxidation, which is in agreement with XPS analysis. Nevertheless, no features related to cobalt oxides can be straightforwardly seen in the spectrum, indicating that oxidized Co atoms are involved in a different type of neighborhood, most likely surrounded by nitrogen and carbon atoms and different geometry. Figure 3c shows the |FT| of the k^2-weighted EXAFS spectra and curve-fittings of Co precursor and **Co@NC-800** samples. Co precursor exhibits quite a strong signal up to around 4 Å divided into three different contributions, testifying the crystallinity and the high degree of order.

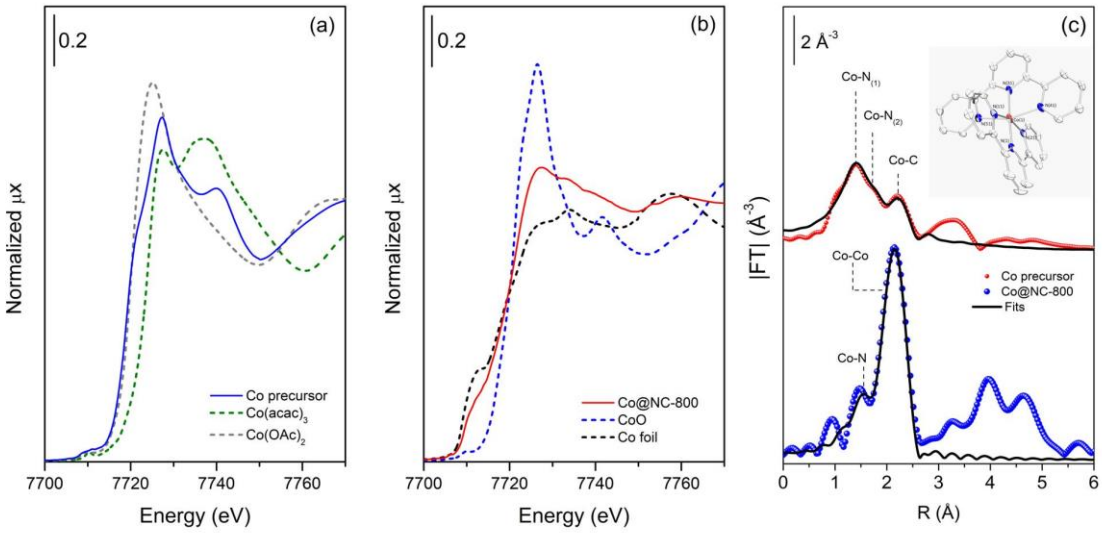

Figure 3. Normalized XANES spectra (a-b) at Co K-edge of Co precursor, **Co@NC-800** and respective Co-based standards with possible similarity to our studied samples. (c) Moduli of Fourier Transform and curve-fittings of Co precursor and **Co@NC-800**.

The Co precursor spectrum was fitted using the crystallographic information (CIF) obtained by single-crystal XRD,[49] which demonstrates to be an excellent model and leads to quite similar results when the two techniques are compared. Since a large number of atoms involved and the significant number of different paths needed to be considered to describe the precursor, as a first step, all paths generated by FEFF starting from this model were summed, giving rise to alike |FT| (Figure S6). After that, a rigid (only four free parameters) fit was also performed considering all summed paths as a model, resulting in a good curve-fitting up to 4Å (Figure S6). Both results demonstrate the excellent model represented by the single-crystal XRD structure and the quality of the precursor compound. In order to perform a quantitative evaluation, a more straightforward fit was performed considering the two first coordination shells. As aforementioned, two different Co-N contributions at 1.4 and 1.7 Å (not phase-corrected) with total N_{Co-N} = 6 and a third (and less accurate) Co-C contribution at 2.2 Å with N_{Co-C} = 5.5 were obtained. **Co@NC-800** displays an intense Co-Co contribution at 2.1 Å with N_{Co-Co} = 5.9, representing Co nanoclusters with a diameter around 0.8 nm, considering a cubooctahedral shape and a narrow particle size distribution.[59,60] Further, it is possible to observe a small shoulder at ~1.4Å that was fitted as a Co-N(O) contribution with N_{Co-N} = 2, which supports the XANES and XPS results on the presence of oxidized Co patches after pyrolysis. This shoulder has already been observed in the literature for a similar system.[30] The quantitative information obtained by EXAFS fittings is gathered in Table S1.

Taking all characterization results together, a geometric confinement of Co nanoclusters within N-doped graphitic carbon shells is proposed. Co nanoclusters are covered by Co-N_x layers, which protect them from over oxidation by air. Moreover, nitrogen in the carbon framework could serve as active sites beneficial for interacting with the functionalized nitroarene substrate by π-π stacking interactions and activating H_2, which was reflected by the difference in catalytic performance with the catalyst in which the activated carbon support was not doped with N, **Co-P_1@C-800**, **Co-P_2@C-800** (Table 1, entries 19, 20).

2.4. Catalytic activity of Co@NC-800.

In order to explore the general catalytic performance of **Co@NC-800** in the synthesis of anilines, a wide range of substituted nitroarenes containing electron-donating and electron-withdrawing groups at different ring positions were tested using the optimized conditions.

Table 2 shows the results obtained for the synthesis of different anilines. The catalytic system is perfectly tolerant for a wide range of functional groups such as halogen-containing substrates. The presence and the position of F, Cl or Br in the aromatic ring did not affect in the catalytic activity and neither the process selectivity. Even with 1-iodo-2-nitrobenzene, a substrate with very sensitive functional group such as iodo, it has been obtained an excellent result. Moreover, no dehalogenation process was observed. In addition, nitroarenes cyano-, hydroxil-, amide- or ester-substituted were tested in the reduction reaction. In all cases, the corresponding anilines were obtained with excellent yields, without any detecting by-products. In addition, the presence of sterically demanding groups in orto position in the aromatic ring did not affect in the catalytic activity or in the process selectivity. Heteroatom-containing anilines are important intermediates in the agrochemical and pharmaceutical industries. In this work, they could be obtained through the corresponding nitroarene reduction with quantitative yields. The reduction of pharmaceutically important substrates such as nitroresorcinol or flutamide have been attempted due to the interest of the corresponding reduction products as key intermediates in the preparation of biologically active compounds.

Table 2. Cobalt-catalyzed hydrogenation of substituted nitroarenes.[a,b]

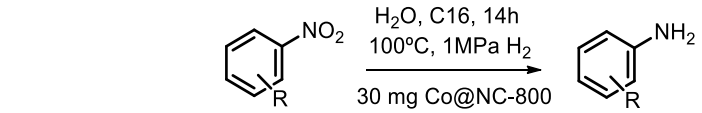

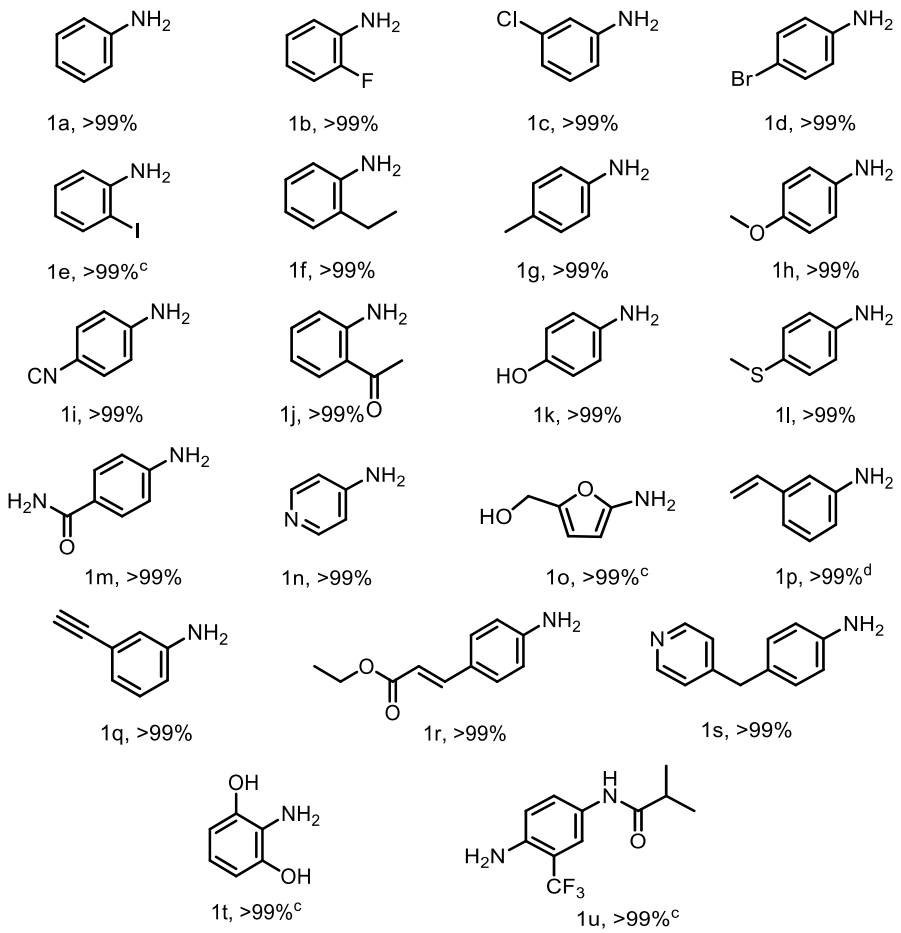

[a]All reactions were performed on 0.5 mmol scale. [b]Conversions were determined by GC-MS analysis of the crude reaction mixture. [c]Ethanol was used as solvent. [d]20h of reaction time.

Interestingly, the nitroarenes containing different reducible functional groups, such as ketone, nitrile, alkene and alkyne groups were reduced entirely to their corresponding aniline products with >99% selectivity, since the other reducible groups remaining untouched, highlighting the excellent chemoselectivity of **Co@NC-800**. Moreover, this catalyst activity (TOF = 11.76 h^{-1}) has been compared with other reported non-noble metal catalysts (Table S2). To achieve similar results to the ones we are reporting in this work organic solvents, high metal loading or pressures are required.

To check the chemoselectivity of the catalyst on the reduction of 3-nitrostyrene, hydrogenation of styrene and nitrobenzene was carried out separately under identical reaction conditions. As shown in Table 2, aniline (1a) was obtained in high yield after 14 hours, while, in the same

time, ethylbenzene was not detected in the GC analysis indicating the preference reduction of the nitro group instead of the vinyl group. Our group has extensively studied this methodology with other catalysts such as Au/TiO_2[15] and Co@C.[19]

In order to demonstrate the preferential adsorption and activation of the nitro group in **Co@NC-800**, an ATR-FTIR study with nitrobenzene and 3-nitrostyrene as probe molecules has been performed. Previously, FTIR studies with these probe molecules have widely been used in our group with different materials containing transition metals.[19,61] The different adsorption modes of nitro and vinyl groups present in the 3-nitrostyrene could be correlated with the chemoselectivity of the process. In all these cases, the asymmetric ν_{as} and symmetric ν_s bands of the nitro group were preferentially detected in the FTIR spectra instead of the ν (C=C) and the δ (=C-H) bands, indicating superior adsorption of the nitro group onto the catalyst and favoring the reduction of this one. In our case, when nitrobenzene was adsorbed onto the catalyst and measured by FTIR spectroscopy (Figure S7), the ν_{as} and ν_s bands of $-NO_2$ were detected at 1523 and 1546 cm^{-1} (Figure 4) that are shifted from pure nitrobenzene on KBr (Figure S7). This is an evidence of the strong interaction of the nitro group in **Co@NC-800**. Moreover, when 3-nitrostyrene was adsorbed onto the catalyst surface, only bands associated with the nitro function are observed (ν_{as} and ν_s at 1527 and 1348 cm^{-1} respectively), indicating the preferential adsorption of the nitro group instead of the vinyl group, (ν(C=C) and δ(=C-H) bands appears at 1636 and 1416 cm^{-1} respectively).[62] The consequence of the preferential adsorption of the nitro group is the chemoselective hydrogenation of 3-nitrostyrene to the corresponding aniline-derivate using **Co@NC-800** as catalyst.

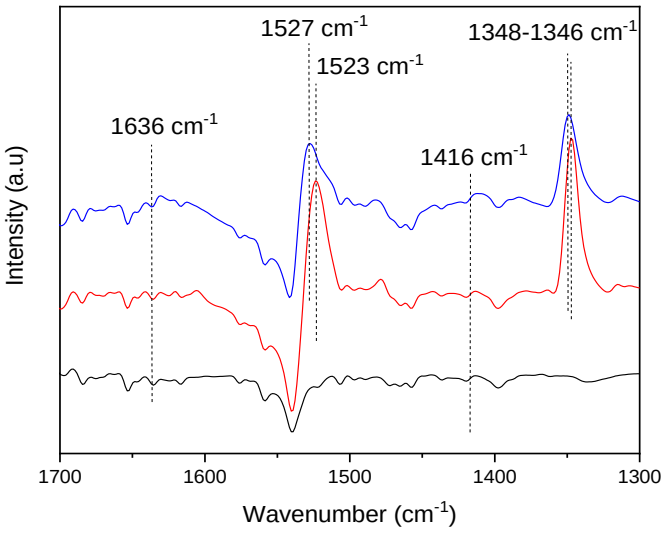

Figure 4. ATR-IR spectra of fresh **Co@NC-800** (black line), and with pre-adsorbed nitrobenzene (red line) and 3-nitrostyrene (blue line).

The stability and heterogeneity of the **Co@NC-800** catalyst were also investigated. Once the nitrobenzene reduction was complete, the catalyst was extracted from reaction media using an

external magnet, then washed with acetone and dried under vacuum at 60 ºC overnight before the next run. As shown in Figure 5a, the catalyst maintains its activity and could be reused at least three times with only a small decrease in activity, maintaining in all cases >99% of selectivity towards aniline. A slight increase of catalyst mass was detected even after a vacuum drying, indicating some residual deposits on the catalyst surface, which cannot be easily removed. To check this hypothesis, after the third run, the catalyst was pyrolyzed at 800 ºC. After this regeneration treatment, the catalyst got back its initial activity completely.

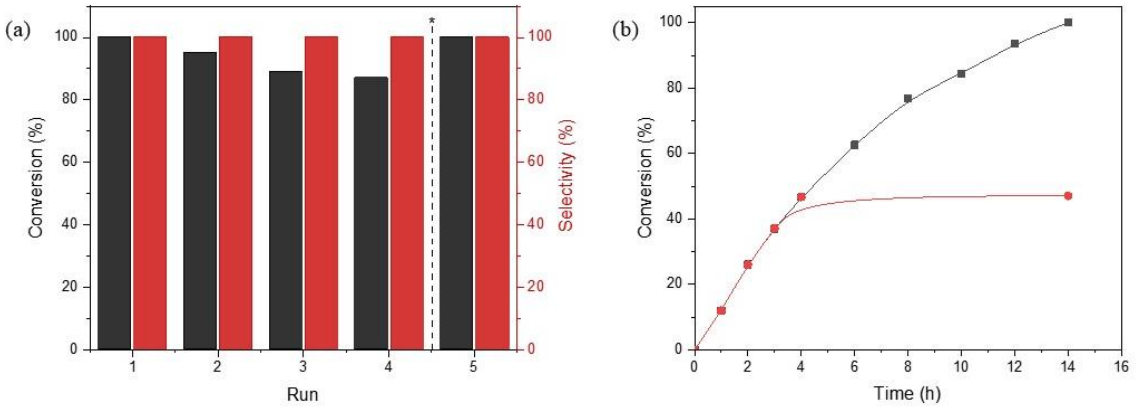

Figure 5. (a) Recycling of **Co@NC-800** catalyst, pyrolysis treatment after the fourth run (dashed line) and (b) hot filtration test of **Co@NC-800** catalyst for catalytic hydrogenation of nitrobenzene to aniline under optimized conditions.

Moreover, a hot filtration test was performed to confirm the heterogeneity of the catalyst (Figure 5b). For that purpose, the reaction was carried out for 4h. After catalyst removal, the resulting filtrate was again held on reaction conditions for 10h. No additional increment of nitrobenzene conversion was detected. The filtrate was analyzed, and Co traces have not been detected by ICP-AES, which indicates cobalt species from the catalyst were not leached to the reaction media and that **Co@NC-800** acts as a true heterogeneous catalyst.

Once proved the general applicability of this catalyst in the reduction of a wide range of nitroarenes, we were interested in tandem transformations, which include a nitroarene hydrogenation step, such as the direct synthesis of secondary amines from nitroarenes and aldehydes. In this cascade reductive amination (Scheme 3), first, the nitro compound must be reduced (A). Then, the rapid formation of an imine should proceed (B), which is then converted to the desired secondary amine through catalytic hydrogenation (C). Moreover, when an aryl aldehyde, such as benzaldehyde, is employed, the final reductive amination product should be intact, avoiding C-N bond cleavage through hydrogenolysis.

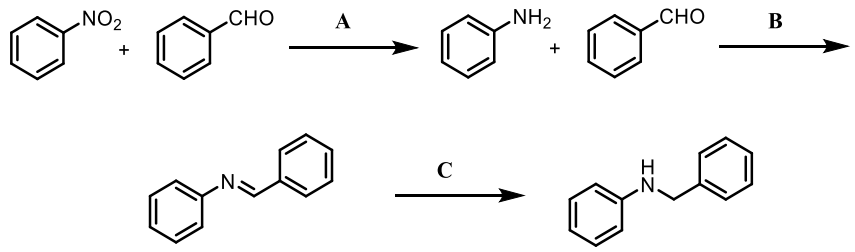

Scheme 3. Cascade reductive amination pathway.

As expected, using **Co@NC-800** as catalyst, the reduction of benzaldehyde under the optimized reaction conditions did not occur. The reductive coupling of several aromatic nitroarenes, containing electron-donating and electron-withdrawing groups, with benzaldehyde was investigated to demonstrate the general applicability of the method (Table 3). Moreover, the selectivity of the process can be controlled by varying the H_2 pressure of the reaction. If the pressure was set to 1 MPa of H_2, the product obtained was the imine, while if the H_2 pressure was increased to 3 MPa, the preferential product obtained was the amine. In conclusion, the selectivity of the process can be controlled by varying the pressure conditions of the process.

Table 3. Cobalt-catalyzed tandem reaction of substituted nitroarenes with benzaldehyde[a,b,c]

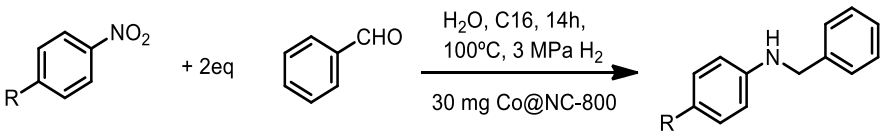

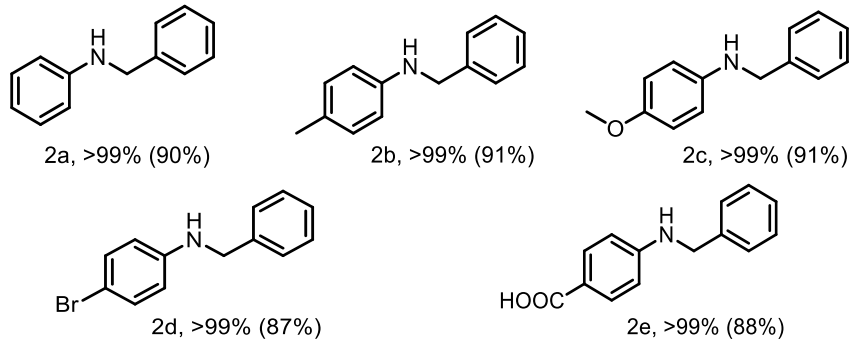

[a]All reactions were performed on 0.5 mmol scale. [b]Conversions were determined by GC-MS analysis of the crude reaction mixture. [c]Isolated yields in brackets.

These results have been compared with other reported heterogeneous cobalt-based catalysts,[28,37,47] resulting that **Co@NC-800** is active under milder reaction conditions than the reported ones. Moreover, in this work, the reductive amination has been carried out in water as a green solvent.

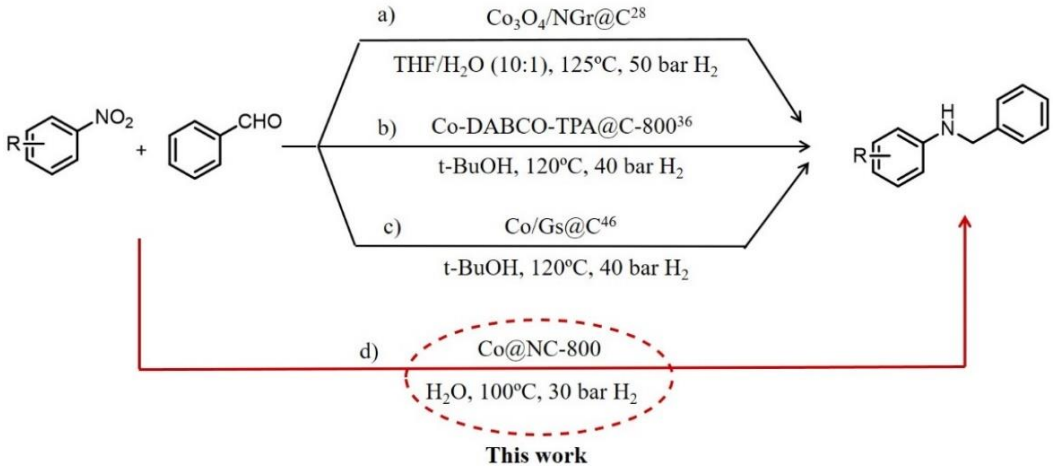

Scheme 4. Reductive amination of nitroarenes over cobalt-based heterogeneous catalysts.

A more straightforward reaction that implies a nitroarene hydrogenation step, the one-pot reaction of nitroarenes and 2-formylbenzoic acid was carried out, which affords in good yield and selectivity the isoinolinones listed in Table 4. As in the previous tandem reaction, the reduction of 2-formylbenzoic acid (alone or with nitrobenzene) under the optimized reaction conditions did not occur and the cascade reaction of variously substituted nitro compounds, containing electron-donating and electron-withdrawing groups, with 2-formylbenzoic acid was investigated to demonstrate the general applicability of the method.

Table 4. Cobalt-catalysed tandem reaction of substituted nitroarenes with 2-carboxybenzaldehyde.[a,b,c]

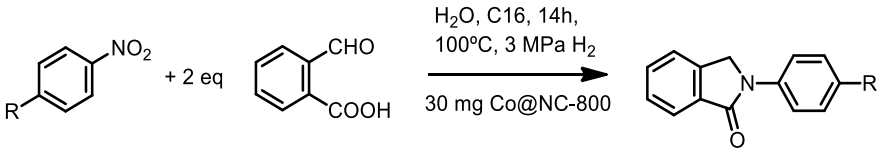

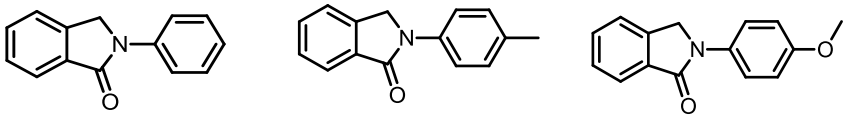

3a, >99% (92%)

3b, >99% (89%)

3c, >99% (90%)

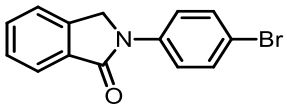

3d, >99% (88%)

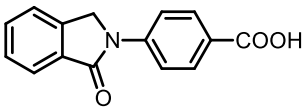

3e, >99% (88%)

[a]All reactions were performed on 0.5 mmol scale. [b]Conversions were determined by GC-MS analysis of the crude reaction mixture. [c]Isolated yields in brackets.

3. CONCLUSIONS

To sum up, we present a strategy for the synthesis of **Co@NC-800**, where metallic Co nanoclusters are stabilized by Co-N_x and covered by layers of *N*-doped carbon as core-shell. These layers protect from over oxidation by air, avoiding the deep oxidation of Co nanoclusters. This catalyst is led by the employment of a suitable molecular complex consisting of six bounds N-Co and a high pyrolysis temperature. The synthesized catalyst showed excellent dispersion of cobalt nanoclusters, which was confirmed by PXRD, HAADF-STEM, EXAFS and other physicochemical techniques. The presence of nitrogen in the graphitic carbon and the polar reaction conditions helps with the heterolytic cleavage of H_2, which was demonstrated by isotopic exchange experiments. Under optimized conditions, a wide range of functionalized nitroarenes was hydrogenated with excellent selectivity under mild reaction conditions and water as a green solvent. In addition, this catalyst was reused for four consecutive runs with a minimum loss of activity, which could be recovered entirely after a pyrolysis treatment of the catalyst and it has not shown cobalt leaching in the reaction media. Furthermore, **Co@NC-800** is highly active for one-pot synthesis of several secondary amines from a variety of nitroarenes and benzaldehyde and for one-pot synthesis of several *N*-aryl substituted isoindolinone derivatives from 1-formylbenzoic acid and several nitroarenes also using water as a solvent. Finally, IR adsorption experiments have been carried out to explain the chemoselectivity of the **Co@NC-800** for the nitro towards the alkene function, considering that the adsorption properties of substrate molecules will be affected by the chemical state of Co. This work provides new insights into the design of non-noble metal catalysts for heterogeneous catalytic applications.

4. ASSOCIATED CONTENT

Experimental Section

Experimental procedures employed during this study, PXRD, Raman spectra, STEM images and characterization of catalytic products are described in the Supporting Information. The Supporting Information is available free of charge on the ACS Publications website.

Notes

The authors declare no competing financial interest.

ACKNOWLEDGMENT

Program Severo Ochoa SEV-2016-0683 is gratefully acknowledged. S.G.T. thanks to MINECO for her FPU Ph.D. contract FPU16/02117. P.O-B. thanks MICCIN for his Ramón y Cajal contract RYC-2014-16620. Authors thank the financial support by the Spanish Government (RTI2018-096399-A-I00). The High-Resolution STEM data were recorded at the DME-UCA

node of the ELECMI ICTS Spanish National Infrastructure for Electron Microscopy of Materials. JJC acknowledges financial support from MINECO/FEDER (Project MAT2017-97579-R). In addition, P.O-B. thanks UPV for his grant PAID-06-18/SP20180172. C.W.L. thanks PRH 50.1 – ANP/FINEP Human Resources Program (Brazil) for the Visiting Researcher Fellowship.

5. REFERENCES

1 R. S. Downing, P. J. Kunkeler and H. Van Bekkum, *Catal. Today*, 1997, **37**, 121–136.

2 Wiley-VCH, *New York*, 2001, 31611.

3 H.-U. Blaser, C. Malan, B. Pugin, F. Spindler, H. Steiner and M. Studer, *Adv. Synthe. Catal.*, 2003, **345**, 103–151.

4 H. U. Blaser, H. Steiner and M. Studer, *ChemCatChem*, 2009, **1**, 210–221.

5 L. L. Santos, P. Serna and A. Corma, *Chem. - A Eur. J.*, 2009, **15**, 8196–8203.

6 A. Corma and P. Serna, *Science (80-.).*, 2006, **313**, 332–334.

7 T. Mitsudome, Y. Mikami, M. Matoba, T. Mizugaki, K. Jitsukawa and K. Kaneda, *Angew. Chemie - Int. Ed.*, 2012, **51**, 136–139.

8 H. Wei, X. Liu, A. Wang, L. Zhang, B. Qiao, X. Yang, Y. Huang, S. Miao, J. Liu and T. Zhang, *Nat. Commun.*, 2014, **5**, 1–8.

9 P. J. C. M. R. Friedfeld, M. Shevlin, J. M. Hoyt, S. W. Krka, M. T. Tudge, *Science (80-.).*, 2013, **342**, 1073–1076.

10 S. Zhang, C. R. Chang, Z. Q. Huang, J. Li, Z. Wu, Y. Ma, Z. Zhang, Y. Wang and Y. Qu, *J. Am. Chem. Soc.*, 2016, **138**, 2629–2637.

11 S. G. Warren, E. Yacoub and G. M. Ghose, *Nat. Commun.*, 2014, **5**, 5643–5655.

12 R. Nie, J. Wang, L. Wang, Y. Qin, P. Chen and Z. Hou, *Carbon N. Y.*, 2012, **50**, 586–596.

13 L. W. Covert, R. Connor and H. Adkins, *J. Am. Chem. Soc.*, 1932, **54**, 1651–1663.

14 F. Chen, C. Topf, J. Radnik, C. Kreyenschulte, H. Lund, M. Schneider, A. E. Surkus, L. He, K. Junge and M. Beller, *J. Am. Chem. Soc.*, 2016, **138**, 8781–8788.

15 A. Corma, P. Serna, P. Concepción and J. J. Calvino, *J. Am. Chem. Soc.*, 2008, **130**, 8748–8753.

16 B. Chen, F. Li, Z. Huang and G. Yuan, *ChemCatChem*, 2016, 1132–1138.

17 G. Melaet, W. T. Ralston, C. S. Li, S. Alayoglu, K. An, N. Musselwhite, B. Kalkan and G. A. Somorjai, *J. Am. Chem. Soc.*, 2014, **136**, 2260–2263.

18 L. Liu, F. Gao, P. Concepción and A. Corma, *J. Catal.*, 2017, **350**, 218–225.

19 L. Liu, P. Concepción and A. Corma, *J. Catal.*, 2016, **340**, 1–9.

20 D. Formenti, C. Topf, K. Junge, F. Ragaini and M. Beller, *Catal. Sci. Technol.*, 2016, **6**, 4473–4477.

21 Y. Liao, Z. Cheng, W. Zuo, A. Thomas and C. F. J. Faul, *ACS Appl. Mater. Interfaces*, 2017, **9**, 38390–38400.

22 P. Zhou, L. Jiang, F. Wang, K. Deng, K. Lv and Z. Zhang, *Sci. Adv.*, 2017, **3**, 1–11.

23 M. Li, F. Xu, H. Li and Y. Wang, *Catal. Sci. Technol.*, 2016, **6**, 3670–3693.

24 N. P. Wickramaratne, J. Xu, M. Wang, L. Zhu, L. Dai and M. Jaroniec, *Chem. Mater.*, 2014, **26**, 2820–2828.

25 Y. Li, J. Zhang, Q. Wang, Y. Jin, D. Huang, Q. Cui and G. Zou, *J. Phys. Chem. B*, 2010, **114**, 9429–9434.

26 F. A. Westerhaus, R. V. Jagadeesh, G. Wienhöfer, M. M. Pohl, J. Radnik, A. E. Surkus, J. Rabeah, K. Junge, H. Junge, M. Nielsen, A. Brückner and M. Beller, *Nat. Chem.*, 2013, **5**, 537–543.

27 D. Formenti, F. Ferretti, C. Topf, A. Surkus, M. Pohl, J. Radnik, M. Schneider, K. Junge, M. Beller and F. Ragaini, *J. Catal.*, 2017, **351**, 79–89.

28 R. V. Jagadeesh, T. Stemmler, A. E. Surkus, M. Bauer, M. M. Pohl, J. Radnik, K. Junge, H. Junge, A. Brückner and M. Beller, *Nat. Protoc.*, 2015, **10**, 916–926.

29 T. Schwob and R. Kempe, *Angew. Chemie - Int. Ed.*, 2016, **55**, 15175–15179.

30 X. Sun, A. I. Olivos-Suarez, D. Osadchii, M. J. V. Romero, F. Kapteijn and J. Gascon, *J. Catal.*, 2018, **357**, 20–28.

31 Y. Y. Tao Song, Peng Ren, Yanan Duan, Zhaozhan Wang, Xiufang Chen, *Green Chem.*, 2018, **20**, 4629–4637.

32 P. Serna and A. Corma, *ACS Catal.*, 2015, **5**, 7114–7121.

33 J. Feng, S. Handa, F. Gallou and B. H. Lipshutz, *Angew. Chemie - Int. Ed.*, 2016, **55**, 8979–8983.

34 C. Yu, X. Guo, Z. Xi, M. Muzzio, Z. Yin, B. Shen, J. Li, C. T. Seto and S. Sun, *J. Am. Chem. Soc.*, 2017, **139**, 5712–5715.

35 A. García-Ortiz, J. D. Vidal, M. J. Climent, P. Concepción, A. Corma and S. Iborra, *ACS Sustain. Chem. Eng.*, 2019, **7**, 6243–6250.

36 A. Garcia-Ortiz, J. D. Vidal, S. Iborra, M. J. Climent, J. Cored, D. Ruano, V. Pérez-Dieste, P. Concepción and A. Corma, *J. Catal.*, 2020, **389**, 706–713.

37 R. V. Jagadeesh, K. Murugesan, A. S. Alshammari, H. Neumann, M. M. Pohl, J. Radnik and M. Beller, *Science (80-.).*, 2017, **358**, 326–332.

38 F. Mao, D. Sui, Z. Qi, H. Fan, R. Chen and J. Huang, *RSC Adv.*, 2016, **6**, 94068–94073.

39 S. Pisiewicz, T. Stemmler, A. E. Surkus, K. Junge and M. Beller, *ChemCatChem*, 2015, **7**, 62–64.

40 H. Kato, I. Shibata, Y. Yasaka, S. Tsunoi, M. Yasuda and A. Baba, *Chem. Commun.*, 2006, 4189–4191.

41 P. Zhou, C. Yu, L. Jiang, K. Lv and Z. Zhang, *J. Catal.*, 2017, **352**, 264–273.

42 X. Cui, K. Liang, M. Tian, Y. Zhu, J. Ma and Z. Dong, *J. Colloid Interface Sci.*, 2017, **501**, 231–240.

43 Y. Z. Chen, Y. X. Zhou, H. Wang, J. Lu, T. Uchida, Q. Xu, S. H. Yu and H. L. Jiang, *ACS Catal.*, 2015, **5**, 2062–2069.

44 P. Zhou and Z. Zhang, *ChemSusChem*, 2017, **10**, 1892–1897.

45 B. Sreedhar, P. Surendra Reddy and D. Keerthi Devi, *J. Org. Chem.*, 2009, **74**, 8806–8809.

46 A. Cho, S. Byun and B. M. Kim, *Adv. Synth. Catal.*, 2018, **360**, 1253–1261.

47 K. Murugesan, V. G. Chandrashekhar, T. Senthamarai, R. V. Jagadeesh and M. Beller, *Nat. Protoc.*, 2020, **15**, 1313–1337.

48 Y. Duan, T. Song, X. Dong and Y. Yang, *Green Chem.*, 2018, **20**, 2821–2828.

49 S. Gutiérrez-Tarriño, P. Concepción and P. Oña-Burgos, *Eur. J. Inorg. Chem.*, 2018,

2018, 4867–4874.

50 A. Martínez, G. Prieto and J. Rollán, *J. Catal.*, 2009, **263**, 292–305.

51 N. A. M. Barakat, B. Kim, S. J. Park, Y. Jo, M. H. Jung and H. Y. Kim, *J. Mater. Chem.*, 2009, **19**, 7371–7378.

52 Y. Hou, Z. Wen, S. Cui, S. Ci, S. Mao and J. Chen, *Adv. Funct. Mater.*, 2015, **25**, 872–882.

53 Z. L. Wang, X. F. Hao, Z. Jiang, X. P. Sun, D. Xu, J. Wang, H. X. Zhong, F. L. Meng and X. B. Zhang, *J. Am. Chem. Soc.*, 2015, **137**, 15070–15073.

54 L. Zhang, P. Hu, X. Zhao, R. Tian, R. Zou and D. Xia, *J. Mater. Chem.*, 2011, **21**, 18279–18283.

55 D. Mhamane, W. Ramadan, M. Fawzy, A. Rana, M. Dubey, C. Rode, B. Lefez, B. Hannoyer and S. Ogale, *Green Chem.*, 2011, **13**, 1990–1996.

56 F. Jaouen, J. Herranz, M. Lefévre, J. P. Dodelet, U. I. Kramm, I. Herrmann, P. Bogdanoff, J. Maruyama, T. Nagaoka, A. Garsuch, J. R. Dahn, T. Olson, S. Pylypenko, P. Atanassov and E. A. Ustinov, *ACS Appl. Mater. Interfaces*, 2009, **1**, 1623–1639.

57 P. Yin, T. Yao, Y. Wu, L. Zheng, Y. Lin, W. Liu, H. Ju, J. Zhu, X. Hong, Z. Deng, G. Zhou, S. Wei and Y. Li, *Angew. Chemie - Int. Ed.*, 2016, **55**, 10800–10805.

58 L. Shang, H. Yu, X. Huang, T. Bian, R. Shi, Y. Zhao, G. I. N. Waterhouse, L. Z. Wu, C. H. Tung and T. Zhang, *Adv. Mater.*, 2016, **28**, 1668–1674.

59 H. Fei, J. Dong, M. J. Arellano-Jiménez, G. Ye, N. Dong Kim, E. L. G. Samuel, Z. Peng, Z. Zhu, F. Qin, J. Bao, M. J. Yacaman, P. M. Ajayan, D. Chen and J. M. Tour, *Nat. Commun.*, 2015, **6**, 1–8.

60 T. Yamamoto, *X-Ray Spectrom.*, 2008, **36**, 27–34.

61 G. Agostini, A. Piovano, L. Bertinetti, R. Pellegrini, G. Leofanti, E. Groppo and C. Lamberti, *J. Phys. Chem. C*, 2014, **118**, 4085–4094.

62 J. M. Montejano-Carrizales, F. Aguilera-Granja and J. L. Morán-López, *Nanostructured Mater.*, 1997, **8**, 269–287.

63 M. Boronat, P. Concepción, A. Corma, S. González, F. Illas and P. Serna, *J. Am. Chem. Soc.*, 2007, **129**, 16230–16237.

64 Y. Tan, X. Y. Liu, L. Zhang, A. Wang, L. Li, X. Pan, S. Miao, M. Haruta, H. Wei, H. Wang, F. Wang, X. Wang and T. Zhang, *Angew. Chemie*, 2017, **129**, 2753–2757.

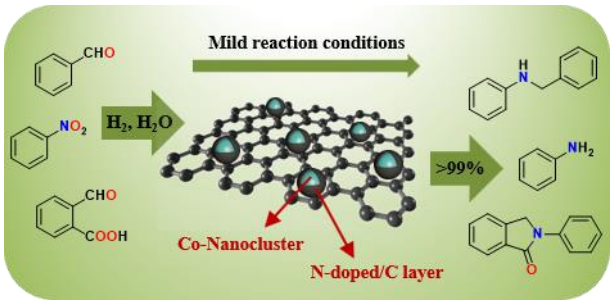

Subnanometric cobalt nanoclusters cover by N-doped carbon layers as core-shell (**Co@NC-800**) catalyzed the chemoselective reduction of nitroarenes and the one-pot synthesis of secondary aryl amines and isoindolinones in aquo media under mild reaction conditions.